

LNF - 67/64
2 Ottobre 1967

G. Baldacchini and V. Montelatici: MEASUREMENTS OF
DYNAMIC POLARIZATION OF PROTONS IN CRYSTALS
AND INSTRUMENTATION. -

(Nota interna: n. 382)

Nota Interna: n° 382
2 Ottobre 1967

G. Baldacchini^(x) and V. Montelatici: MEASUREMENTS OF DYNAMIC POLARIZATION OF PROTONS IN CRYSTALS AND INSTRUMENTATION. -

(This work will be presented at the "Conference of S.I.F., Bologna (Ottobre 1967)).

SUMMARY. -

This report is a preliminary study of dynamic polarization of protons in the hydration water in $\text{La}_2\text{Mg}_2(\text{NO}_3)_{12} \times 24 \text{H}_2\text{O}$ crystals doped with paramagnetic impurity of Nd^{3+} . This effect occurs when a microwave source saturates the transitions that simultaneously flips a proton and a Nd^{3+} ion. The work is intended only to detect the "effect solide" on two crystals with different concentrations of Nd^{3+} ions at the LARMOR frequency of about 24 KMc/s and in the temperature range of $1 \div 4^\circ\text{K}$. The dependence of polarization, whose maximum value was about 20%, on the pumping power was measured as well as the two signs of polarization and proton relaxation times. The instrumentation developed for the experiment and concerning both a narrow band system and a periodic wide band system is described.

(x) - C.N.R. fellowship, 1966.

2.

1. - DYNAMIC POLARIZATION BY "EFFECT SOLIDE". -

1.1. - Qualitative explanation of the effect. -

The "effect solide", which may occurs in the double resonance phenomena, will be described qualitatively; for a deeper understanding we shall refer to the specialized literature. The effect is based on the dipole-dipole coupling between magnetic moments: those associated with the spin angular momentum of two different types of spins. It was discovered, first, for the case of the nuclear-nuclear coupling case by Abragam and Proctor on 1958⁽¹⁾, and for the case of electron-nuclear coupling a by Erb et al.⁽²⁾ in the liquids on the same year; it was extended to solids by Abraham et al. on 1958⁽³⁾ and by Leifson and Jeffrie⁽⁴⁾ on 1961.

In our laboratory, we observed this effect in a single diamagnetic crystal of $\text{La}_2\text{Mg}_3(\text{NO}_3)_{12} \times 24\text{H}_2\text{O}$ with paramagnetic impurities. We shall, therefore, study the dynamic polarization of protons in such a crystal, which may be represented from a magnetic point of view as formed by paramagnetic ions S of Neodinium and by protons I of the crystallization water molecules. The Nd^{3+} ion has a angular momentum $\hbar\vec{S}$ with effective spin $|S| = 1/2$, and magnetic momentum $-g\beta\vec{S}$. This model may be assumed to be adequate since the highest temperature is 4°K ⁽⁵⁾. The Landè g factor, because of the spin-orbit-crystal field coupling, depends on the angle, θ , between the axis the crystal and the magnetic field direction.

$$g(\theta) = (g_{\parallel}^2 \cos^2 \theta + g_{\perp}^2 \sin^2 \theta)^{1/2}$$

with $g_{\parallel} = 0.362$ and $g_{\perp} = 2.702$ ⁽⁵⁾

The dipolar energy is negligible compared to the Zeeman energy when the spins are in an external field greater than a few hundred Gauss; thus the energy levels for the (I, S) pair are:

$$E(M_S, m_I) = g_S \beta M_S H_0 - g_I \beta m_I H_0 = |\gamma_S| \hbar H_0 M_S - \gamma_I \hbar H_0 m_I$$

where γ is the gyromagnetic ratio of ions, ($\gamma_S < 0$) and protons ($\gamma_I > 0$). As shown in Fig. 1 the usual allowable transitions are that for which the selection rules $\Delta m_I = 0$, $\Delta m_S = \pm 1$ and $\Delta M_S = 0$, $\Delta M_I = \pm 1$ are valid.

The dipolar magnetic coupling between \vec{S} and \vec{I} at distance \vec{r} ,

$$H_{dd} = - \frac{g_S g_I \beta^2}{r^3} \left[\vec{I} \cdot \vec{S} - \frac{3(\vec{I} \cdot \vec{r})(\vec{S} \cdot \vec{r})}{r^2} \right]$$

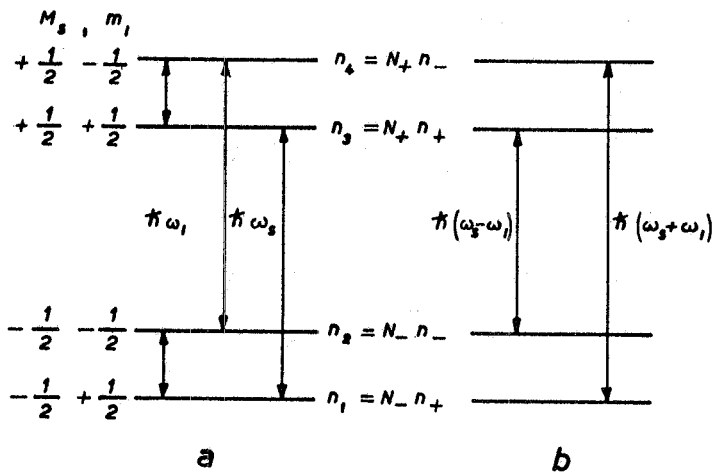


FIG. 1 - Energy levels; unperturbed states M_S, m_I ; n_i = mean occupation number of the level of energy E_i ; N_i and n_i are mean occupation number of the electrons S and proton I in the state (+) or (-), a) allowed transitions, b) forbidden transitions.

mixes partially the energy levels through its non-diagonal terms, so that there is a relaxation probability $w \approx \alpha w_s \neq 0$ (with $\alpha = (\gamma_S \hbar / r^3)^2 \cdot H_0^2$ and w_s = electron transition probability) between levels for which $\Delta M_S = \pm 1, \Delta m_I = \pm 1$. Therefore the transitions between the states (4, 1) and (3, 2), normally forbidden, are thus permitted. The resonance spectrum of the crystal, in our schematization, has a finite intensity at the frequency $\omega_{1,2} = \omega_s \pm \omega_I$, $\omega_3 = \omega_s$, $\omega_4 = \omega_I$. We suppose that the three lines of the ionic spectrum are resolved completely. Then an electromagnetic field of frequency, e.g. $\omega_1 = \omega_I + \omega_s$, will induce the transitions between the levels (4, 1); the level populations have mean occupation number different from Boltzmann equilibrium after reaching the stationary state. If moreover the nuclear relaxation process is slower than that induced at frequency ω_1 , and this second process, on its turn, is slower than the electronic relaxation process, the electronic population ratio is not modified from its Boltzmann equilibrium. When the saturation condition ($n_4 = n_1$) is satisfied, the nuclear population ratio is:

$$(1) \quad \frac{n_+}{n_-} = \left(\frac{N_+}{N_-} \right)_0$$

where the subscript 0 refers to the case of Boltzmann equilibrium.

We shall use the relation ⁽⁶⁾ between the difference of the chemical potentials of the levels 4 and 1 and the ratio of the probability of the thermal relaxation (w) to probability of induced relaxation (W) to obtain, qualitatively, the behaviour of polarization as a function of the power at the frequency ω_1 :

$$\Delta \mu \equiv \mu_4 - \mu_1 = \frac{E_4 - E_1}{1 + w/W} \equiv (E_4 - E_1) s$$

where $E_4 - E_1 = \hbar H_0 (|\gamma_S| + \gamma_I)$ and s is a saturation parameter. This parameter depends on the amplitude of alternate magnetic field of the pumping power; for $s = 0$, or $W = 0$, $\Delta \mu = 0$ and $s = 1$, or $W \rightarrow \infty$, $\Delta \mu = \hbar H_0 \cdot (|\gamma_S| + \gamma_I)$. The ratio $n_4/n_1 = N_+ n_- / N_- n_+$, as a function of $\Delta \mu$ is

4.

$$\frac{N_+ n_-}{N_- n_+} = \exp \frac{\Delta\mu - (|\gamma_s| + \gamma_I) \mu H_0}{K T}$$

where T is the heat bath temperature. Keeping in mind the relation (1), one obtains, from the last relationship:

$$\frac{n_-}{n_+} = \exp \left(\frac{|\gamma_s| \mu H_0}{K T} \right) \exp \left[\frac{(s-1)(|\gamma_s| + \gamma_I) \mu H_0}{K T} \right]$$

Since the polarization, for $|I|=1/2$, is defined as

$$p = \frac{n_+ - n_-}{n_+ + n_-}$$

one has:

$$(2) \quad p = \pm \operatorname{tanh} \left\{ - \frac{\mu H_0}{2 K T} \left[|\gamma_s| + (s-1)(|\gamma_s| + \gamma_I) \right] \right\} \approx \pm \frac{\mu H_0}{2 K T} \left[|\gamma_s| + (s-1)(|\gamma_s| + \gamma_I) \right]$$

where the lower sign applies to the case of a pumping at the frequency $\omega_2 = \omega_s - \omega_I$; now, since the system S is antiparallel to external field, also p must have the same direction: therefore p gives rise to an emission signal, corresponding to an inverted nuclear population. Obviously this is an ideal case: it does not consider some effects which reduce the value given by formula (2). We suppose the three lines of electronic spectrum extremely sharp so that one can saturate a line without producing interference with the others. The best condition is $\omega_I \gg \Delta\omega$, where $\Delta\omega$ is the electronic line-width; in this case the two forbidden transition $(\omega_s \pm \omega_I)$ are separated from each other and from the allowed electronic transition ω_s ; in this case an electromagnetic field can induce a selective saturation. If this is not the case, the spin dynamics involves different spin temperatures including one for the spin-spin interaction energy; and different cases occur depending on the origin of the line width, which can be homogeneous or inhomogeneous; in this last situation, the dynamic polarization depends on the thermal equilibrium between the electronic spins having slightly different resonance frequencies.

The use of high magnetic field and substances with resolved lines is the optimum obtainable in this respect. A more rigorous treatment of dynamic polarization shows a dependence of p on a leakage factor $\left[1 + (n/N)(T_S/T_I) \right]^{-1}$ (4) which reduces the ideal value (n and N are the number of protons and electrons, T_I and T_S the corresponding relaxation

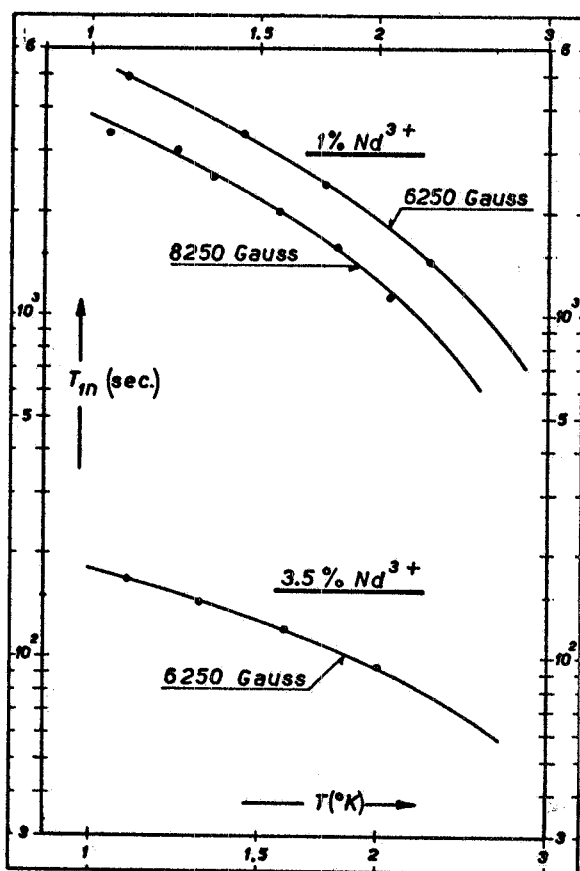


FIG. 2 - Proton relaxation time T_{1n} obtained observing the proton signal decay after switch off the microwave pumping power, at the labelled magnetic field as function of the temperature.

time spin-lattice). Because of the weak coupling one must have $n > N$. This unfavourable condition is balanced with T_S many order less than T_I when the concentration of ion is low, for ex. 1%. A concentration of 3.5% reduces T_I more than an order of magnitude and reduces the polarization, Fig. 2. The concentration of electronic spins should be sufficiently high, so that the electronic spins can have an effective action on the proton spin. The maximum usable concentration is limited by the increase of the line width because of the spin-spin interaction and because of the onset of phonon bottle-neck effect.

This phenomenon depends on the scarce number of phonons at such low temperature; they are not able to transfer the energy received from paramagnetic ions to the heat bath. Consequently the lattice temperature (which is the temperature of importance for the protons), reaches a value higher than the heat bath temperature. Thus the protons remain at a high temperature, and the polarization is reduced.

The electronic relaxation times should not be too short otherwise the dynamic polarization would require higher microwave power, and the phonon bottle-neck effect can occur; on the other hand, they should not be too long otherwise the mechanism of the polarization is not effective.

The leakage factor should be near the unity, and this is not always the case in various substances. On this respect the double nitrate crystals are particularly useful. The typical values are:

$$\frac{n}{N} > 10^3, \quad T_S \simeq 10^{-4} \text{ sec}, \quad T_I \simeq 10^3 \text{ sec.}$$

allowing for a polarization comparable to ideal value to be reached. Due to the low concentration of paramagnetic ions, one spin S polarizes only

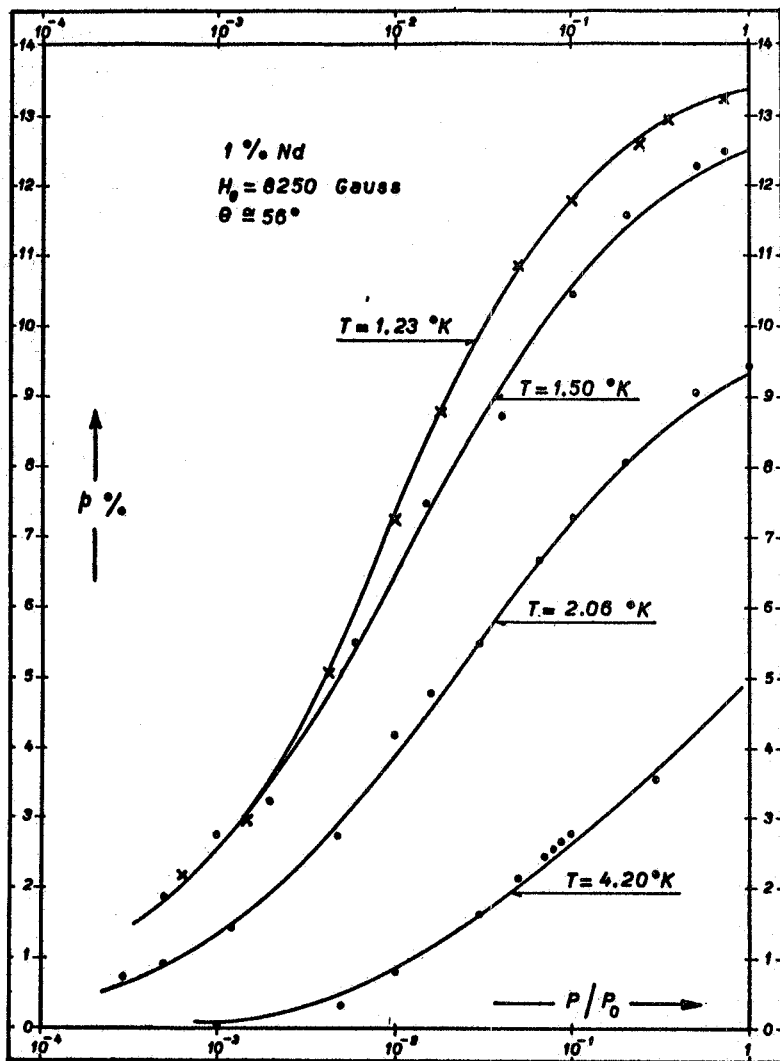


FIG. 3 - Dynamic polarization of protons in the hydration water molecules of the double nitrate, Nd^{3+} concentration 1%. Dependence of polarization on pumping power at different temperature.

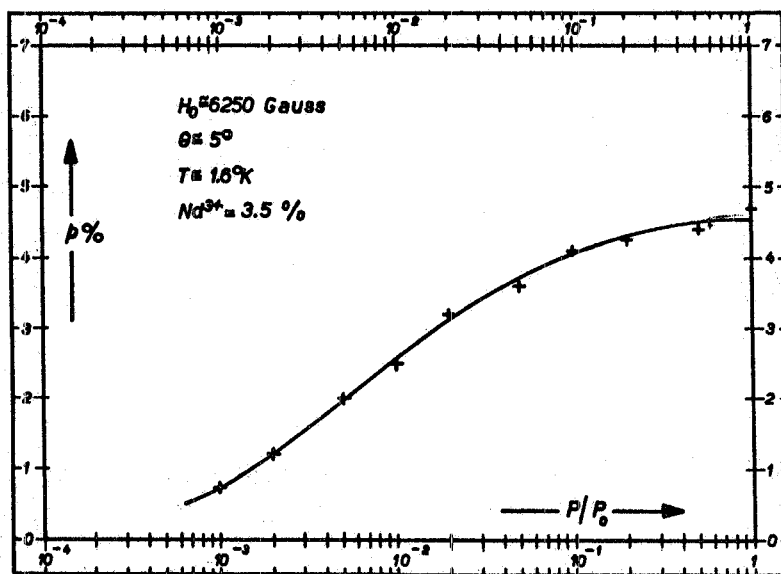


FIG. 4 - Nd^{3+} concentration 3.5%, dependence of polarization on pumping power, note the reduction in the protons polarization.

a few spins I, the nearest neighbour, and a diffusion effect transports the polarization from one spin I to the other. The spin I, strongly polarized, through the proton-proton dipolar interaction induces transitions on the nearest spin, which, on its turn, induces again polarization on the next spin, and so on. Since these mutual inductions conserve the energy, rapidly a transport process polarizes all the spins of the crystal.

1.2 - Measurements. -

The measurements are performed in magnetic fields of 8250 Gauss and 6250 Gauss, correspondingly to the LARMOR frequency of 35500 Kc/s and 26500 Kc/s for protons and 23990 Mc/s and 23300 Mc/s for electrons, on two crystals of $\text{La}_2\text{Mg}_3(\text{NO}_3)_{12} \times 24\text{H}_2\text{O} + 1\%$, (3.5%), Nd^{3+} , (4.10^{22} protons/cm³ and 7.10^{22} nuclei/cm³).

The polarization dependence on the pumping power is shown in Fig. 3, 4. Such a dependence is observed to be in agreement with formula (2). The maximum polarization value $p=0.18$, is compared with the ideal value $p=0.55$ for $T=1^\circ\text{K}$ and $f_s=24000$ Mc/s. This large difference shows the presence of effects reducing the polarization. The Fig. 5, 6 show the

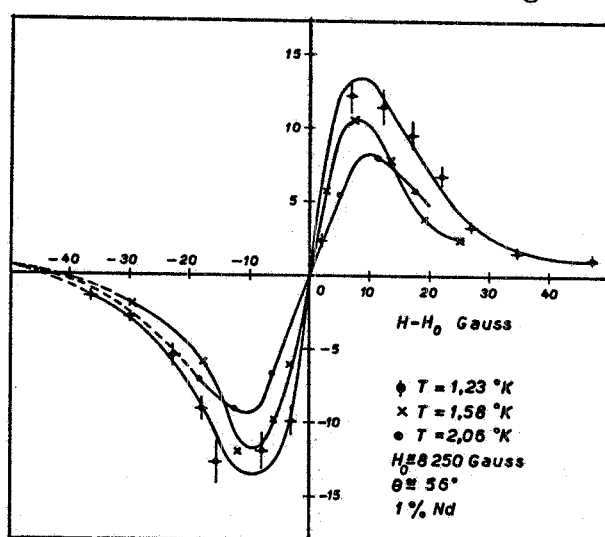


FIG. 5 - Dynamic polarization at constant power as function of the magnetic field at different temperatures; Nd^{3+} concentration 1%.

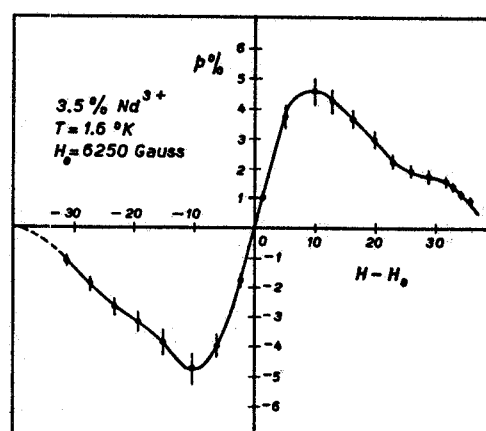


FIG. 6 - Dynamic polarization at the same power of Fig. 5 but with a 3.5% Nd^{3+} concentration.

two signs of polarization as a function of the magnetic field at different temperatures and for two different ion concentrations. The curves of Fig. 7 give the polarization as a function of temperature for two magnetic fields. It can be noted that at the higher field the polarization is lower. This is due to a less resolved spectrum at 8 KGS with respect to the

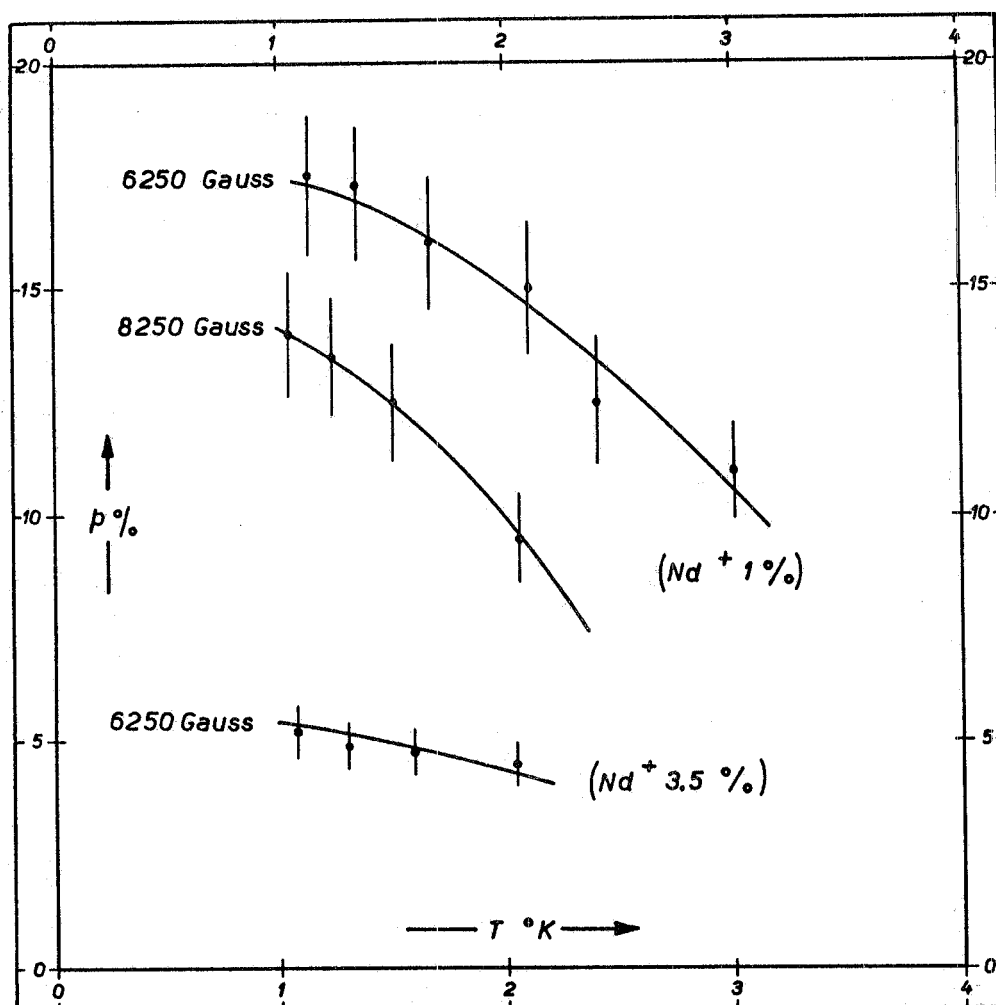


FIG. 7 - Dynamic polarization as function of temperatures different magnetic fields and concentration.

spectrum of 6 KGS. In both cases there is no selective pumping. The worst resolution at 8 KGS is due to a wider line at $\theta = 56^\circ$, compared with the line at $\theta = 90^\circ$ corresponding at the 6 KGS resonance. Moreover it is noted that at about 1.5°K . the saturation behaviour of the polarization does not follow the $1/T$ dependence. This is due primarily to the onset of phonon bottle-neck.

The single crystals^(x) are grown from a saturated solution of $\text{La}_2\text{Mg}_3(\text{NO}_3)_{12} \times 24\text{H}_2\text{O}$ in which 1% of the La ions is replaced by Nd^{3+} .

(x) - The chemical components have the following sources. Lanthanum nitrate, purity 99.997, and Neodymium nitrate purity 99.9 from American Potash of Chemical Corporation, Magnesium nitrate analytical reagent from Mallinckrodt.

They are grown in a desiccated atmosphere in a temperature bath at about 0°C.

First, a solution a lanthanum magnesium nitrate is made up by mixing the proper amounts of lanthanum nitrate and magnesium nitrate, adding enough water to bring the solution below the saturation level at 0°C. Then the solution is doped with the proper amount of neodymium nitrate. The solution is then brought to saturation and it is placed in a flat cup. In a few days a great many small crystals begin to form, and those which have the most perfect hexagonal shapes are kept as seeds from which to grow large crystals.

The good seeds are placed in individual cups so that they are able to grow.

The Nd ions appear not to crystallize as readily as La ions, and it is estimated that crystals grown from 1% doped solution contain only about 0.2% Nd(x).

2. - MAGNETIC RESONANCE APPARATUS. -

The instrumentation to detect the electronic and proton resonances consists of two spectrometers: one for the electronic resonance at high frequency, about 24000 Mc/s and one for the proton resonance variable from 20 to 40 Mc/s.

The frequency of the klystron reflex (OKI, 24 V 11; output power $\simeq 0.5$ Watt) is kept constant and the magnetic field is varied to cross the resonances at $H_0 = 2\pi f_s / \gamma_s(\theta)$ and $H_0 = 2\pi f_I / \gamma_I$, where f_s and f_I are the LARMOR frequency.

2.1. - Detection of electronic resonance. -

A direct wide band detection is sufficient to observe the electronic resonance. This technique consists of a modulating magnetic field (at 50c/s) superimposed on H_0 and observing the power absorbed from the cavity. The Fig. 8 gives the block diagram; the derived branches are used to monitor the power supplied from the oscillator and the paramagnetic absorption signal reflected from the cavity. The resonant cavity is continuously tunable to cross the working frequency with a movable piston; a stub above the coupling iris matches the guide with the cavity. Generally the matching conditions are different at the various temperatures. The cavity, of which a detailed study was made⁽⁹⁾ previously, oscillates on a single a mode, the TE_{011} one, at the frequency f_s . It is cut at half way through an orthogonal plane to its axis; between the two pieces

(x) - Private communication from Gilbert Shapiro.

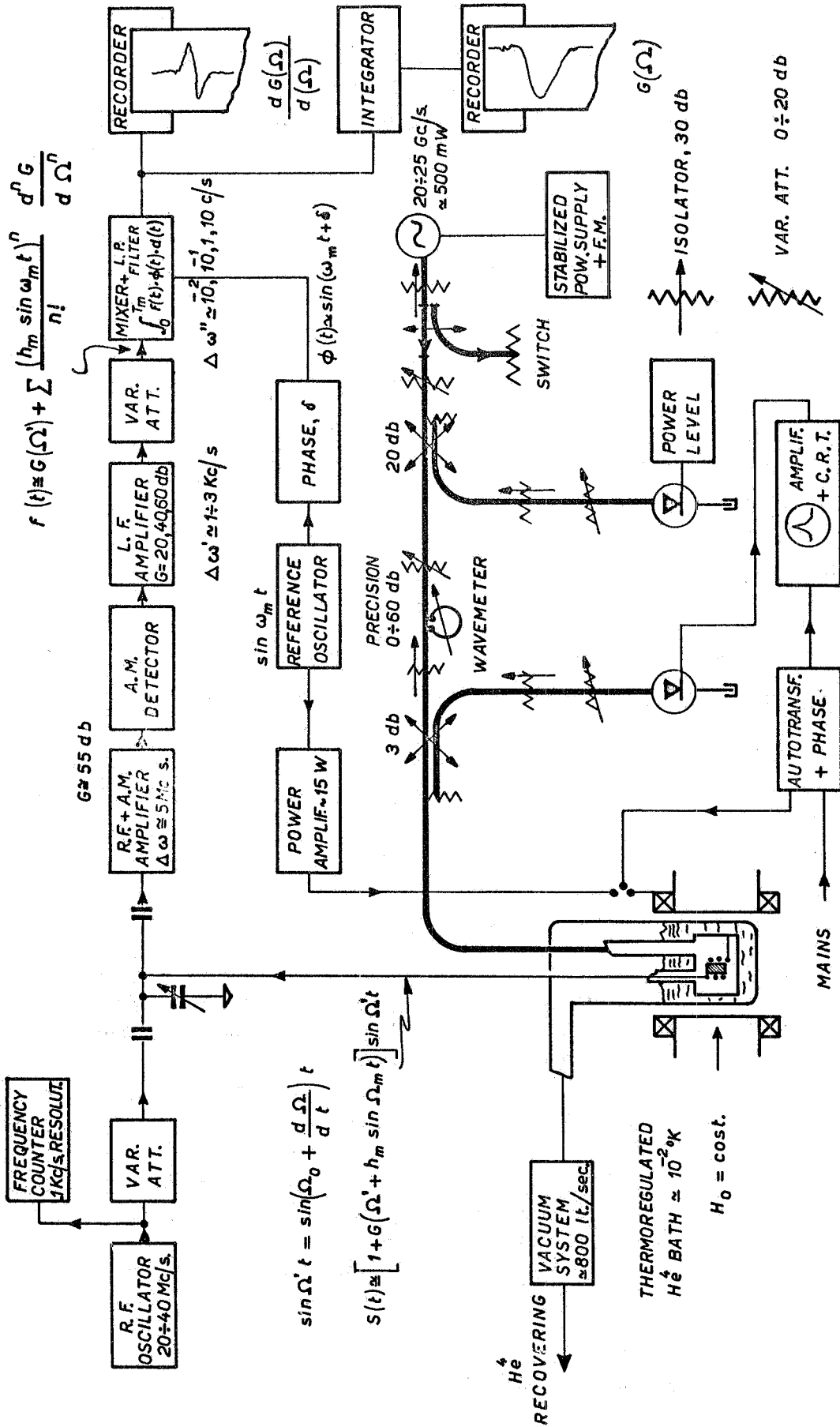


FIG. 8 - Block diagram of the detection systems of the proton and electron magnetic resonances.

there is adapted a mylar sheet (thickness 2 mills). In this way the induced currents on the cavity from an external modulating field of high frequency (1 Kc/s + 50 Kc/s) are strongly reduced. The figure of merit of the silvered cavity is not reduced appreciably since the cut is parallel to the very high frequency currents on its internal surface; its value with the sample inside is about 10.000 at low temperatures. The Fig. 9 shows the cavity drawing with the rods to move the piston and the matching stub. The upper flange is screwed on a metallic support, the vacuum inside is obtained by an "O" ring. A Glass dewar is adapted to the support and its lower end is placed between the pole pieces of the magnet, which has a gap of about 8 cm. The magnet is energized with a d. c. power supply which gives variable currents from 0 to 120 A. (0 - 100 Volt) with a stability of 1 part on 10^5 on short range. The homogeneity on the sample is better than 10^{-4} .

A pumping system, with about 800 lt/s pumping speed, enables to reduce the vapour pressure of the Helium bath to reach a final temperature of about 1°K. The bath is thermoregulated with an electronic system at lower temperatures, and with a mechanical one at higher temperatures, to about 10^{-2} °K.

2.2. - Detection of proton resonance. -

The proton magnetic resonance is detected by using two methods: both a narrow band and a wide band system. Both systems enable to detect the variations of potentials to the ends of a L, C parallel circuit, which is tuned at the proper frequency and fed by a constant current oscillator. The potential variations are proportional to the impedance variations. When the potential variations Δv (due to inductance variations caused by magnetic resonance of the magnetic moments) are small compared with the potential v_0 , then:

$$\frac{\Delta Z}{Z_0} = \frac{\Delta v}{v_0} = -4\pi\eta Q \chi''$$

where χ'' is the imaginary part of the dynamic susceptibility which gives rise to the absorption, η a factor near to unity which depends on the geometry of the L coil and on the linear dimensions of the sample, Q is the quality factor of the circuit. When χ'' has values that brings the ratio $\Delta v/v_0$ near 1, this approximation is no more valid, and corrections must be made.

Both methods are a detection systems under rapid passage through resonance. Since the crossing time of the resonance is shorter than the spin-lattice relaxation time and longer than spin-spin relaxation time one has:

$$T_1 \frac{\dot{H}}{H_1} \gg 1$$

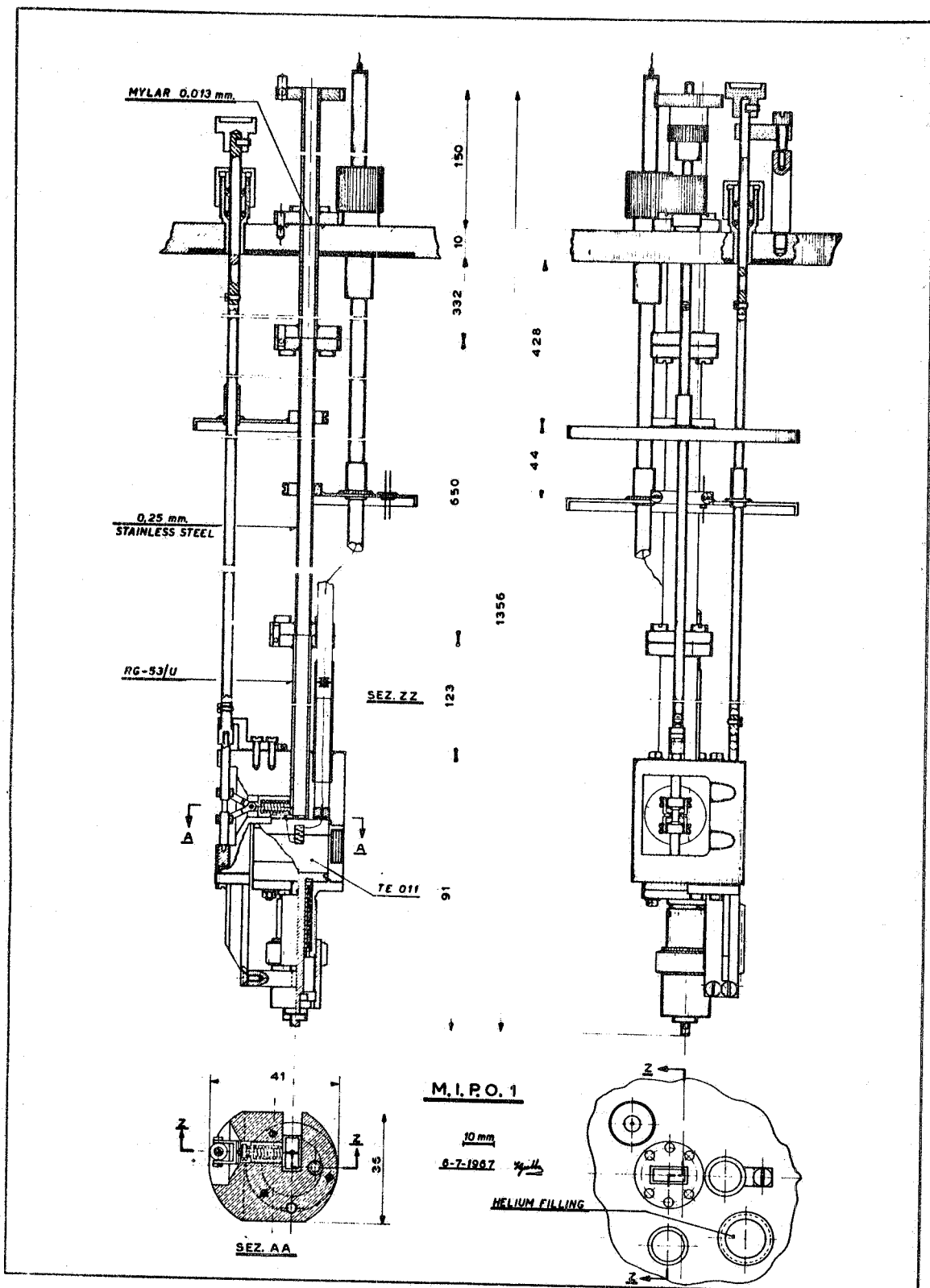


FIG. 9 - Drawing of the resonant cavity working in the helium bath.

where \dot{H} is the variation on time of the magnetic field, H_1 the amplitude of the oscillating magnetic field inside the detection coil.

The narrow band detection (see Fig. 8) is performed by fixing the magnetic field at the proper value, while the frequency is varied linearly to cross the resonance line. On the same time a modulation magnetic field is superimposed to H_0 at a frequency of several cycles, with a much less amplitude than the width of the resonance line. The obtained signal is the product $v = h_m \sin \omega_m t \cdot dG(\Omega)/d\Omega$ where $G(\Omega)$ is the shape of the line of resonance, $h_m \sin \omega_m t$ is the modulating field. Mixing this signal with that of reference, a d. c. voltage, proportional to $h_m (dG(\Omega)/d\Omega) \cdot \cos \delta$ (where $\cos \delta$ is the phase between the sinusoidal waves), is obtained. In condition when $\cos \delta \approx 1$ one can observe the function $dG(\Omega)/d\Omega$ or, after integration, the function $G(\Omega)$ (see Fig. 10), displayed on the recorder.

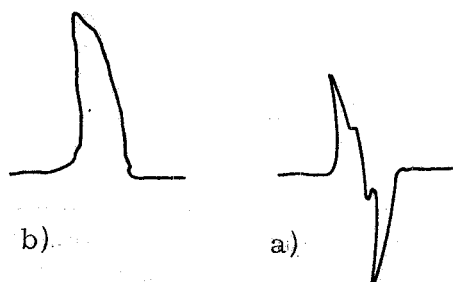


FIG. 10 - Proton resonance under pumping power, 10% polarization; signal as seen after narrow band detection; a) derivative of the b) signal.

The periodic method consists in sweeping the frequency linearly with a saw tooth, on the top of the signal from the resonant circuit, at a repetition of T_0 sec, during t_0 sec.

In this way the alternating field H_1 is t_0/T_0 times lower, compared to the continuous operation and the resonance signal is not saturated. So it is possible to rise the level of the potential difference applied to the sample coil improving the ratio signal to noise. The field H_1 has to be of the order of a fraction of 10^{-3} Gauss to avoid saturation effect. After amplification of the modulated R. F. signal the amplitude-modulation signal is detected. The response is to a good approximation, an arch of parabola which is the image of the resonance curve at the top of the oscillating circuit. The magnetic resonance signal is superimposed on this arch. A signal of the same amplitude and shape is subtracted to this response, so that on the oscilloscope an approximately rectilinear base line is displayed on which the proton magnetic resonance signal is superimposed, Fig. 11 and 12. The sensibility of the narrow band method is by far better. Since the proton resonance signal without pumping is buried in the noise, (the crystal volume is about 100 mm^3) we have used the narrow band method to detect it. On the other hand the periodic method is

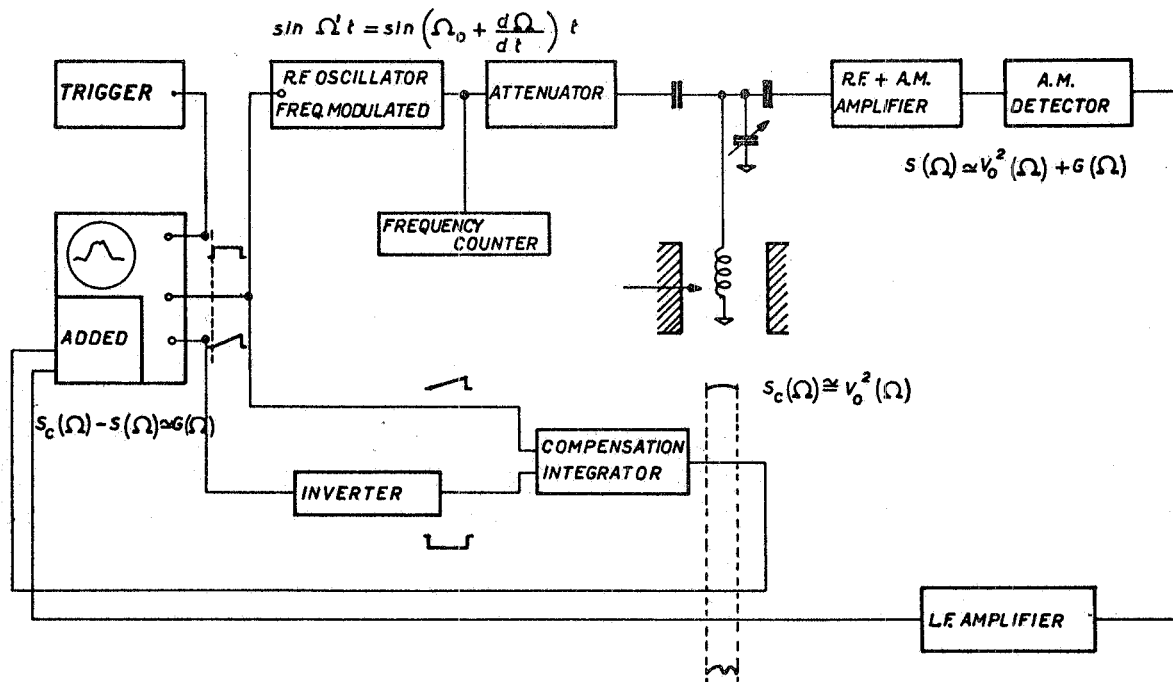


FIG. 11 - Block diagram of the recurrent method.

sufficient to detect signals amplified by pumping. In this way the measurements are rapid and easy to observe. However, a long time is required to permit proton signal reaching dynamic equilibrium. The measure of polarization is performed measuring the susceptibility of the sample $\chi = \chi' - j\chi''$. The polarization is related to the imaginary part of susceptibility by the relation:

$$p = A \int_0^{\infty} \chi'' d\Omega$$

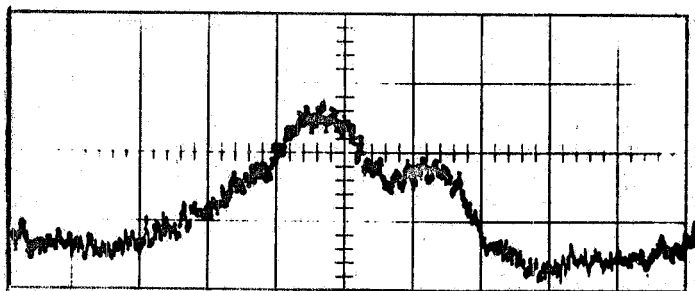
where A is constant physical properties of the sample.

Experimentally one observes the variations of the impedance modulus of the oscillating circuit, which is:

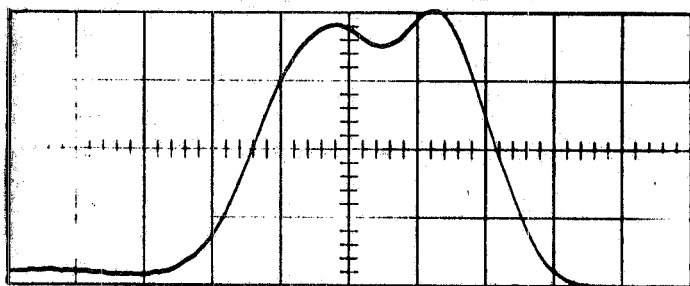
$$Z = \left[\frac{1 + \phi/Q}{r + j\omega L(1 + 4\pi\eta\chi)} + j\omega C \right]^{-1}$$

Its modulus is:

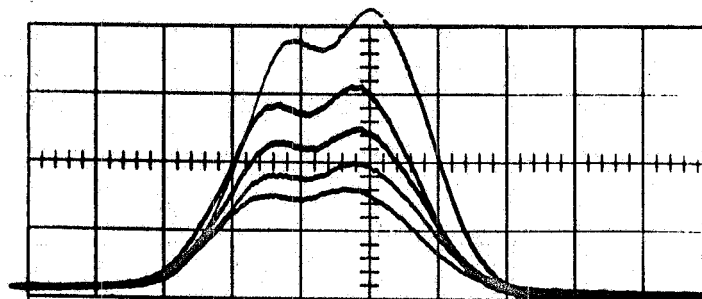
$$|Z| = \omega L \left[\frac{(Q + 4\pi\eta Q \chi')^2 + (1 + 4\pi\eta Q \chi'')^2}{(1 + 4\pi\eta Q \chi'')^2 + (4\pi\eta Q \chi')^2} \right]^{1/2}$$



a) - 0.7% polarization, gain made equal 1



b) - 14% polarization, gain 30 times less



c) - decay of the signal after switch off microwave power to measure the relaxation time, the photos are switched on every 10 minutes.

FIG. 12 - Oscilloscope photography of the proton signals, the trace is ≈ 200 Kc/s.

16.

and if $Q \gg \Phi = 4\pi\eta Q\chi'$, $\varphi = 4\pi\eta Q\chi''$ (generally $Q \approx 50$; $\Phi > 1$, $\varphi < 1$) one obtains:

$$|Z| = R \frac{1 + \Phi/Q}{[(1+\varphi)^2 + \Phi^2]^{1/2}} \approx \frac{R}{1+\varphi} \left[1 - \frac{1}{2} \frac{\Phi^2}{(1+\varphi)^2} \right]$$

with $R = Qr$. The reduced impedance $(|Z_0| - |Z|) \cdot |Z_0|^{-1}$ gives the observed variation, and, dropping terms of order higher than φ^2 and Φ^2 , one obtains:

$$\frac{v_0 - v}{v_0} = \varphi + \frac{1}{2} \frac{\Phi^2}{(1+\varphi)^2}$$

The polarization p , relative to the natural polarization p_0 is given by:

$$p = \int \frac{\Delta v}{v_0} d\Omega \left[1 - \frac{1}{2} \frac{\overline{\Delta v}}{v_0} \right] \frac{p_0}{\int \left(\frac{\Delta v}{v_0} \right)_0 d\Omega} = p_0 \frac{S}{S_0} \left(1 - \frac{1}{2} \frac{\overline{\Delta v}}{v_0} \right)$$

where:

$$p_0 = 2.36 \times 10^{-5} \frac{f_0 \text{ (Mc/s)}}{T_0 \text{ (°K)}}$$

$S_0 = \int (\Delta v)_0 d\Omega$ the corresponding signal, $s = \int \Delta v d\Omega$ the signal amplified by pumping, and $\overline{\Delta v}/v_0$ the maximum percentage variation which is observed on the value v_0 when crossing the resonance; this correction term is due to the non linearity of the Q-meter for high value of φ and Φ . Thus for negative signals (or positive) of polarization, one observes a value of p higher (or lower) than the real one, and the correct value is given by:

$$\frac{p}{p_0} = \frac{S}{S_0} \left(1 \pm \frac{1}{2} \frac{|\Delta v|}{v_0} \right)$$

with upper sign for $p > 0$ and lower one for $p < 0$, which is the expression we have used to obtain the polarization quoted.

3. - SOME CONSIDERATIONS. -

The described method to obtain high polarizations has been applied to the construction of polarized proton targets for scattering experiments. Abragam and Borghini et al. in 1962 built a target which was

used with a 20 MeV proton beam to measure the spin correlation parameter in the p-p scattering in Saclay. This was the first experiment performed with a 20% polarized protons of the hydration water molecule in crystals.

Chamberlain et al. at Berkeley on 1963 where able to increase the dimensions of the target, which was a crystal of $2.5 \times 2.5 \times 2.5 \text{ cm}^3$ with a polarization of about 75%. In many experiments of scattering, the authors showed the usefulness of such a crystal although it contains only 3% by weight of protons obviously the counting technique becomes complicated to avoid spurious effects.

The effect solide to enhance the proton polarization in nuclear targets is of great interest, but also it is of importance in the study of properties of solid state physics. By now the substances investigated in condition of high polarization are not too many, and the phenomenon is under studies.

We note that the work on organic compounds is just at beginning, and that such substances as $C_n H_{2n}$ seem to be very promising as targets for experiments in high energy particles physics.

ACKNOWLEDGMENTS.

It is a pleasure to thank Mr. I. Giabbai and R. Bolli who constructed the low temperatures cavity; Mr. A. Vietti who developed the electronic devices used in our experiments; Mr. I. Cenciarelli for his assistance during the operations at low temperatures.

REFERENCES. -

- (1) - A. Abragam, N.G. Proctor, *Compt. Rend.* 246, 2253 (1958).
- (2) - J. Ubersfield, J.L. Motchane, E. Erb, LXXXVI Colloques Internat. de la Recherche Scientifique.
- (3) - M. Abraham, M.A.H. Causland, F.N.H. Robinson, *Phys. Rev. Letters* 2, 449 (1959).
- (4) - O.S. Leifson, C.D. Jeffries, *Phys. Rev.* 122, 1781 (1961).
- (5) - P.L. Scott, C.D. Jeffries, *Phys. Rev.* 127, 32 (1962).
- (6) - V. Montelatici, *Nuovo Cimento* 47, 104 (1967).
- (7) - P.G. de Gennes, *J. Phys. Chem. Solids* 7, 345 (1958).
- (8) - J.A. Giordmaine, F.R. Nash, *Phys. Rev.* 138, A1510 (1965).
- (9) - G. Baldacchini, V. Montelatici, *Int. Rep. LNF-65/32* (1965).

For the references of the techniques employed we remark only general books since the large literature avoid the possibility to mention every author. Also we mention the recent work by M. Borghini, P. Roubean, C. Ryter.

- C.P. Poole, E.S.R. 1967 (Interscience Publ., London, 1967).
- Sucher, Fox, Handbook of Microwave Measurements, (Politechnic Press of Inst. of Brooklyn, New York, 1963).
- Borghini et al., *Nuclear Instr. and Method* 49, 249 (1967).